energies

MDPI

Article

Analysis of the Parameters of the Two-Sections Hot Side Heat Exchanger of the Module with Thermoelectric Generators

Mirosław Neska *,†, Mirosław Mrozek †, Marta Żurek-Mortka † and Andrzej Majcher †

Łukasiewicz Research Network—Institute for Sustainable Technologies, 26-600 Radom, Poland; miroslaw.mrozek@itee.lukasiewicz.gov.pl (M.M.); marta.zurek-mortka@itee.lukasiewicz.gov.pl (M.Ż.-M.); andrzej.majcher@itee.lukasiewicz.gov.pl (A.M.)

* Correspondence: miroslaw.neska@itee.lukasiewicz.gov.pl

† These authors contributed equally to this work.

Abstract: One of the methods of converting thermal energy into electricity is the use of thermoelectric generators (TEG). The method can be used in low-temperature waste heat conversion systems from industrial installations, but its serious limitation is the low efficiency of thermolectric generators and the relatively low power of the electric waveforms obtained. Increasing the obtained power values is done by multiplying the number of TEGs used, grouped into modules (MTEG). In such systems, the design of the module is extremely important, as it should ensure the best possible heat transfer between both sides of the TEG (hot and cold), and thus obtaining maximum electrical power. The article presents an analysis of a two-section flat plate heat hot side exchanger MTEG. The key parameters like effectiveness of exchange and MTEG efficiency and their impact on the efficiency of heat use and generated electric power were indicated. The tests showed an improvement in these main system parameters for the mixed cycle (co-current and countercurrent—inward direction) of the hot side heat exchanger, compared to the countercurrent flow in both sections of this exchanger.

Keywords: thermoelectric generators; heat exchangers; waste heat; thermocouple

Citation: Neska, M.; Mrozek, M.; Żurek-Mortka, M.; Majcher, M. Analysis of the Parameters of the Two-Sections Hot Side Heat Exchanger of the Module with Thermoelectric Generators. *Energies* **2021**, *14*, 5169. https://doi.org/10.3390/en14165169

Received: 6 July 2021
Accepted: 18 August 2021
Published: 21 August 2021

1. Introduction

One of the elements of sustainable development is the use of solutions for more efficient use of energy. An example of such activities is the closing of technological cycles and the recovery of waste heat energy through its conversion into electricity with the use of thermoelectric generators [1,2]. These systems use thermoelectric phenomena: Seebeck, Thompson, and Peltier effects [3]. Advantageous features of this type of solutions are, i.e., long service life, reliable commissioning, no moving parts, and no maintenance required. This is an advantage of thermogenerators over conventional electricity generation systems. Nevertheless, solutions of this type still have areas for improvement, and one of the main ones is to increase the efficiency of thermal energy conversion into electricity [4], which is currently at the maximum level from 5% to 8% [5]. In laboratory systems, even values of about 10% are achieved [6]. Improving its performance was investigated based upon, among others, the cost-per-watt, power-per-area, and manufacturing quality factor [7].

TEGs are composed of a series of interconnected thermocouples, using the Seebeck effect; they are characterized by the direct generation of electricity from heat. A single cell is composed of two semiconductor elements that conduct electricity and heat. The materials that constitute them characterize a given cell, and they can be materials of the following type: Bi_2Te_3 [8] or Zn_4Sb_3 [9]. Despite the constant search for more effective materials for thermocouples, their conversion efficiency is still relatively low; however, the application to convert low-quality thermal energy into electricity is gaining more and more interest [10–12]. The main challenge of thermoelectric technology remains the improvement of materials' properties and a decrease in costs and commercialization [13].

Since single thermoelectric generators are low-power systems, in order to obtain

higher electric power at the output of the energy recovery system, TEGs are combined into larger sets of generators. Thus, shaping the required output values of the electrical circuit parameters takes place, such as current and voltage.

A typical thermoelectric generator module (MTEG) consists of the following components: a hot side heat exchanger (HSHE), which is designed to provide heat energy from a heat source (HS); a set of thermoelectric generators (THM) and a cold side heat exchanger (CSHE), which works as a heat sink that dissipates the thermal energy of the system (Figure 1).

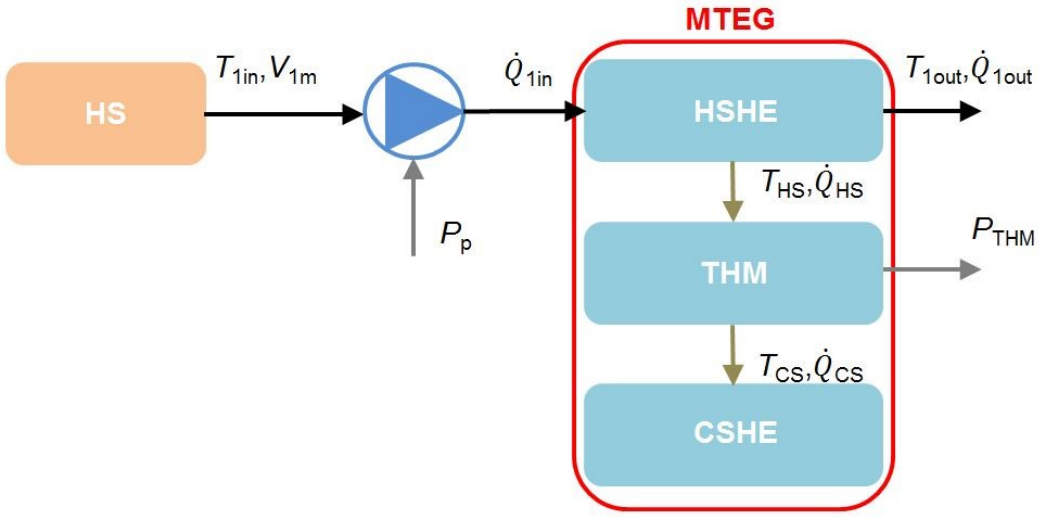

Figure 1. Heat flux distribution in the MTEG system with the thermoelectric modules.

To achieve the maximum possible efficiency of such a system, it is necessary to optimize the geometric and thermodynamic parameters of its individual elements. Garud et al. [14] developed a model of a finned heat exchanger, which was subjected to a combined numerical electro-thermo-structural analysis, and the results were compared with the experiment, optimizing its parameters. The choice of the heat exchanger structure is connected on the one hand with the choice of the heat transfer medium (liquid or gas) [15], and on the other hand with the fluid flow geometry. Esart et al. [16] analyzed selected exchanger geometries: spiral, zig-zag, straight fins. Modeling of the three geometries of exchangers for MTEG allowed for stating that the highest temperature difference of the flowing fluid and the pressure drop can be obtained for the "zig-zag" structure. The mentioned internal geometry solutions or other internal structures (such as: dimple-shaped, maze-shaped, chaos-shaped [5] or fishbone-shaped [17]) can be used in exchangers of various external shapes: hexagonal, tubular, or flat plates.

Numerical analysis of the heat exchanger solution in the form of a flat, parallel plate [18] revealed that the fluid temperature change between the cold and hot part in MTEG is almost linear, while, in traditional plate heat exchangers, it is logarithmic.

Analyzing the literature, it appears that most modules with thermogenerators are made in the automotive industry, where car exhaust fumes are the hot medium. Fewer solutions use a liquid medium. In the area of low-temperature heat energy recovery, the most similar solution was identified in the form of the numerical model presented in Figure 2. The study of this simulation model of a single-section flat plate heat exchanger showed better heat exchange efficiency for counter-rotating flow in relation to concurrent flow. A copper heat exchanger was used for the tests and water was used as the heat exchange medium. In [19], the authors conducted simulation studies of the air gap blocking effect on heat exchange under periodic flow conditions in a plate-fin heat exchanger with a symmetrical cross-section. They showed that blocking the flow of heat through the air gap leads to a reduction in the rate of heat transfer.

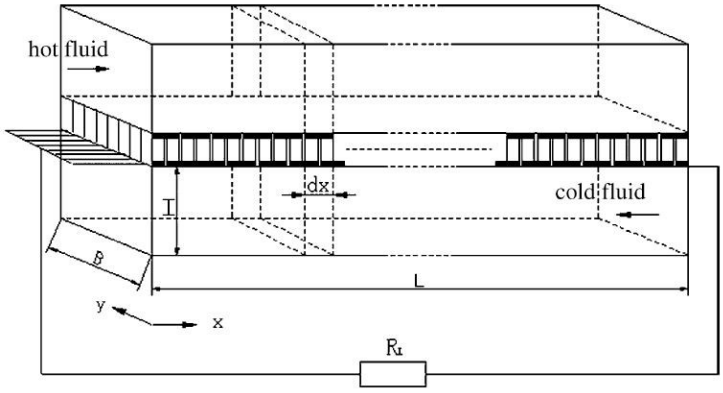

Figure 2. Numerical model of a flat plate finless heat exchanger MTEG. Reprinted with permission from ref. [18]. Copyright 2021 Elsevier and Copyright Clearance Center.

By analyzing the mentioned numerical models of exchangers and low-temperature application solutions [1–20], the MTEG system was developed, with a flat exchanger and with an internal fluid flow geometry similar to "zig-zag", to achieve the greatest possible temperature difference, the possibility of using low-temperature waste heat transferred by liquid, and the modularity and scalability of the solution with the sectional nature of the places of heat energy supply.

The aim of the conducted research is to analyze and compare various configurations of the liquid circulation in the two-section flat plate heat exchanger of the MTEG hot side, with the constant circulation on the cold side. It allows for determining the influence of thermal and flow parameters as well as circulation configuration on the effectiveness of heat use and generated electric power. In addition, the authors included guidelines for the design and optimization of the parameters of the liquid HSHE exchanger for low-temperature heat recovery.

The paper consists of three sections: in the first section, the construction of the TEG module with the dimensions is shown. In the second section, the laboratory stand with the selected parameters of the TEG modules is described. The last part shows the results from the experimental studies of TEG modules with efficiency calculations of the heat exchanger and energy conversion in TEG.

2. Materials and Methods

2.1. The Construction of the TEG Module

The design of the thermoelectric generator module is shown in Figure 3. The main element of the system is a flat, two-section MTEG hot side heat exchanger. The main dimensions of the HSHE are: length 680 mm and width 200 mm (Figure 4), which gives an area to accommodate 20 TEGs.

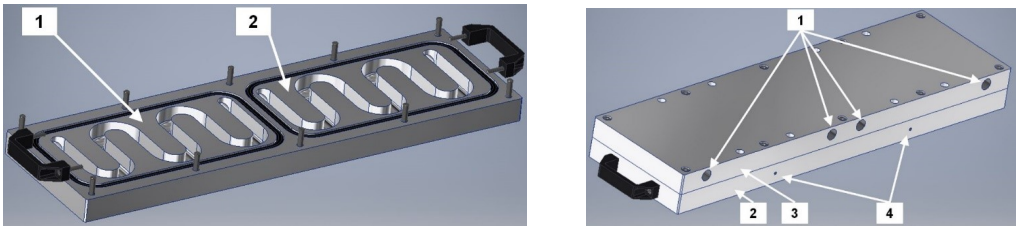

(**a**) (**b**)

Figure 3. Design of two-section MTEG hot side heat exchanger; (**a**) view of the fluid circulation channels, 1—section I, 2—section II; (**b**) assembly view of the exchanger model, 1—channel exit location, 2—intermediate plate, 3—plate with channels, 4—temperature measurement points on the cover plate.

In the analyzed solution, a similar exchanger was used as a CSHE module, which acts as a heat sink to remove heat from the system.

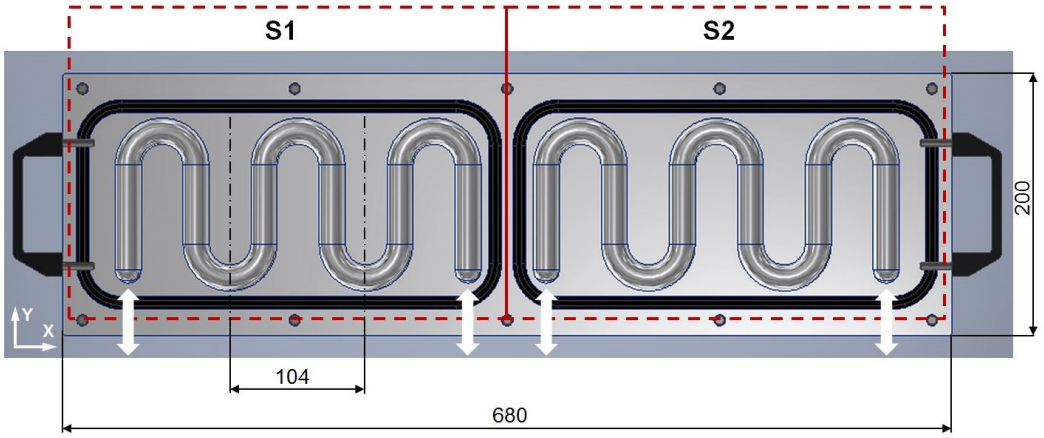

Figure 4. Dimensions of a two-section plate with fluid circulation channels (S1, S2—exchanger sections).

Thermoelectric generators were placed symmetrically, 10 for each section of the exchanger (from $a_{1\,1}$ to $a_{2\,10}$), which are depicted in Figure 5. Between the two-section plate and the THM walls, an intermediate plate was placed, whose task is, on the one hand, sealing the channels, and, on the other, stabilizing the temperature distribution on the surface of single TEGs.

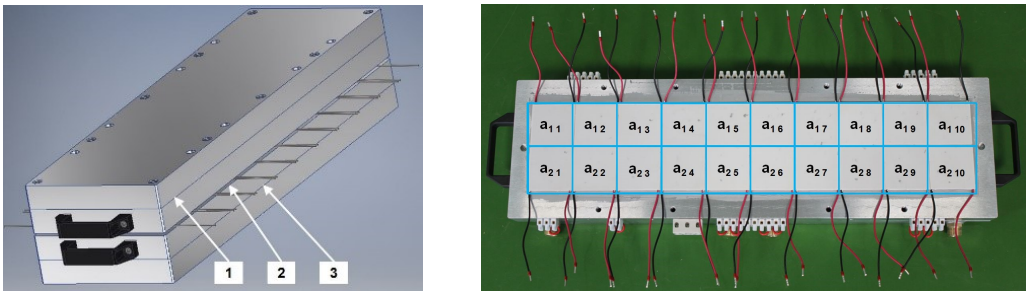

(**a**) (**b**)

Figure 5. MTEG view with arrangement of individual TEGs; (**a**) model (1—hot side exchanger, 2—TEG layer, 3—cold side heat exchanger); (**b**) hot side exchanger prototype with THM.

The presented MTEG is dedicated to receiving thermal energy from industrial installations, for example hot industrial surfaces, from where, through a liquid medium, thermal energy in the form of low-temperature energy is transferred to the MTEG hot side exchanger.

2.2. Description of the Laboratory Stand

The main elements of the MTEG test stand are shown in Figure 6.

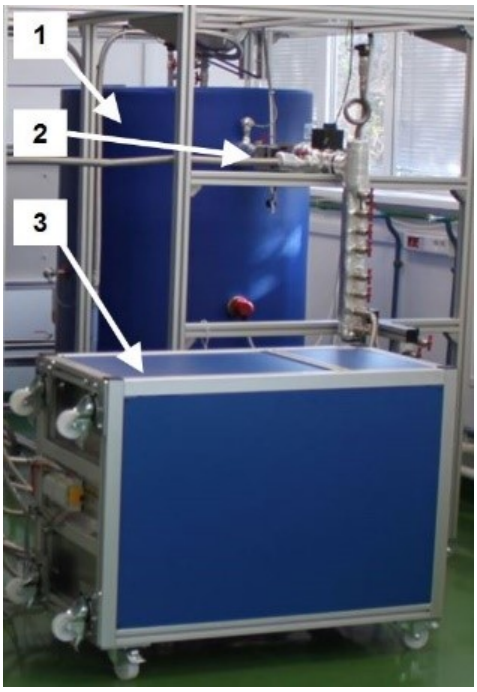

Figure 6. View of the experimental stand with the MTEG: 1—waste heat source with adjustable parameters, 2—connections with a pump, 3—MTEG in a thermally insulated housing.

It allows for testing the parameters of the hot side heat exchanger with a forced flow of fluid with adjustable temperature parameters. In the analyzed system, water was used as the working fluid and thermoelectric modules based on bismuth alloys (Table 1).

Table 1. Selected parameters of the thermoelectric modules MTEG, own elaboration based on [20,21].

Parameter	Value
Dimensions of the module	62 × 62 × 3.9 mm
Number of modules	20
Surface area of internal side of the heat exchanger	1332.8 cm^2
Current of the generated power	2.52 A
Voltage of the generated power	1.84 V
Resistance of the module ($T = 50\,^{\circ}C$)	0.31 Ω
Max. power of the module ($\Delta T = 80\,^{\circ}C$)	4.63 W
Total max. electric power of modules	92.6 W
Max. operating temperature	138 °C
P–N Junction	127 couples

The tests involved effective liquid cooling of the CSHE module at a constant V_{CSHE} flow and T_{CSHE} temperature (Table 2). This approach enables the independent analysis of each of the main elements of MTEG: THM, HSHE, and CSHE. All MTEG components are designed for specific operating parameters. The experimental tests were carried out with different values of V_{1m} and T_{1in} of the hot fluid.

In the system with MTEG, one of the losses are hydraulic losses Δp, resulting from the supply of thermal energy to the THM. In the analyzed solution, these losses constitute the required power P_p for the operation of an additional pump. This power can be considered as an additional load. Other losses in the tested system are heat losses through the HSHE and CSHE casing and connections. Heat transfer is assumed only through the HSHE surfaces in contact with THM. The remaining surfaces were covered with a layer of thermal insulation, hence they were considered adiabatic in the research. The tests did not take into account the heat loss through the HSHE casing to the environment. Aluminum was used as the material for HSHE and CSHE.

Table 2. Selected parameters of the components of the tested system.

Component/Parameter	Material/Medium	Description/Value
heat exchanger	aluminum alloy	dimensions: 680 × 200 × 68 mm, mass: ≈25 kg
V_{1m}	water	0.200 – 0.335 kg/s
T_{1m}	water	60 – 90°C
HSHE circulations	water	variable flow directions: TEG_O1, TEG_O2, TEG_O3, TEG_O4
HSHE sections		S1, S2
V_{CSHE}	water	≈0.335 kg/s
T_{CSHE}	water	9 – 22°C
CSHE circulations	water	constant
CSHE sections		S1, S2

In the analyzed HSHE, four cases of hot fluid circulation were considered (Figure 7).

According to the developed algorithm of the research method (Figure 8), the experiment was carried out for a hot side exchanger with flows parallel to the cold side and circulation configurations: concurrent (TEG-O1), inward (TEG-O2), countercurrent (TEG-O3) and from the center (TEG-O4). The tests were carried out with the same geometrical dimensions of the exchanger and thermophysical parameters of the TEG semiconductors. The influence of the hot fluid flow direction on the temperature distribution and the effectiveness of heat use were compared. In each of the hot side circulations, the speed of the fluid flow was additionally controlled. In the exchanger of the cold side, one circulation and a constant, equal speed of the coolant flow were established.

The algorithm used allowed for the analysis of 42 parameters of the system as a function of three variables (liquid flow direction, initial liquid temperature, liquid flow), with a two-second parameter sampling step and a duration of a single iteration of approximately 30 min.

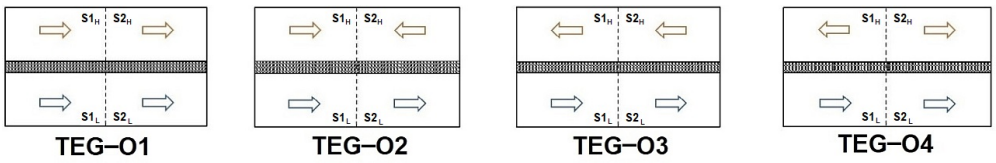

Figure 7. Hot (H) and cold (L) side fluid circulation configurations in the MTEG heat exchanger.

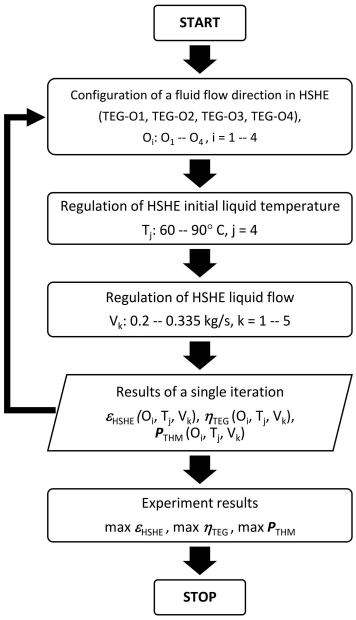

Figure 8. The algorithm of the experiment to analyze the parameters of the MTEG system.

3. Results

3.1. Effectiveness of the Heat Exchanger

HSHE effectiveness was determined using the Carnot dependence, indicating the efficiency of heat transfer. The dependency is defined as:

$$\varepsilon_{HSHE} = \frac{\dot{Q}_1 - \dot{Q}_2}{\dot{Q}_1} = \frac{T_1 - T_2}{T_1} \quad (1)$$

The analyzed effectiveness relates to the heat flowing from one medium $\dot{Q}_1 = \dot{Q}_{1in}(T_1 = T_{FH})$ to another $\dot{Q}_2 = \dot{Q}_{HS}(T_2 = T_{HS})$. Figure 9 shows the dependence of the effectiveness of selected circulations of hot fluid flow via HSHE on the mass flow rate.

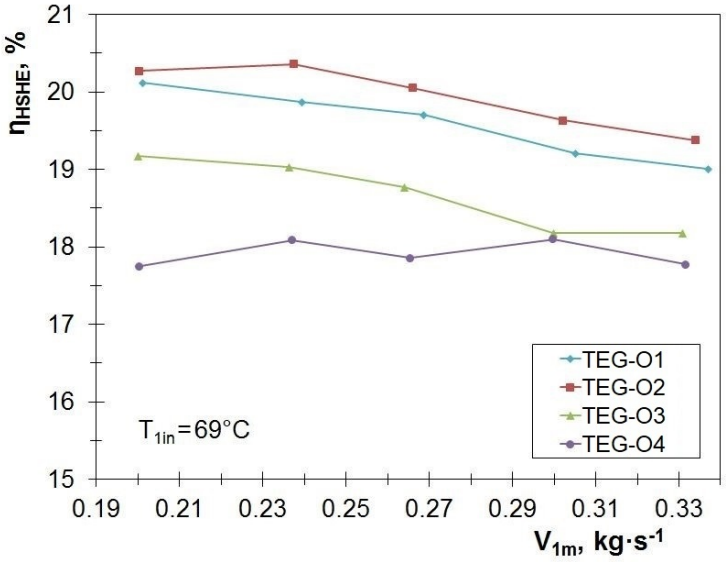

Figure 9. HSHE effectiveness for selected circulations at $T_{1in} = 69\,^{\circ}\mathrm{C}$.

The highest effectiveness of heat exchange was achieved for the TEG-O2 and TEG-O1 circulations. The lowest one was obtained for the TEG-O4. The maximum effectiveness values for these cases were about 20%. This value is about four times lower than in typical exchangers of domestic heating boilers with a capacity of less than 25 kW [22]. In these exchangers, the aim is to minimize the thermal resistance of the partitions between working fluids, hence the effectiveness will be higher. On the other hand, in the MTEG heat exchangers, additional thermal resistance results from the use of thermoelectric modules and a reduced heat exchange surface. This lowers the HSHE effectiveness, and at the same time has a positive effect on the increase of the temperature difference between the hot and cold side of single TEG and more efficient generation of electricity at the THM output.

In the analyzed cases, the value of ε_{HSHE} decreases with the increase of the mass flow rate, which may be due to the decrease in the heat transfer time and the transfer of heat energy between the hot working fluid and the surface of the HSHE channels. Additional effectiveness gains can be made by extending the flow path or changing the geometry of the channels to cause turbulent flow.

The effectiveness determined for the circulations is in correlation with the mean inlet (T_{FH}) and outlet (T_{HS}) temperatures of the MTEG hot side heat exchanger. The lower temperature at the T_{HS} outlet for individual measurement points was obtained for the TEG-O2 (Figure 10), which corresponds to the highest HSHE effectiveness (Figure 9). The relations between the temperature of T_{FH} and T_{HS} are almost linear, hence it follows that the heat transfer coefficient of the fluid is constant in the analyzed temperature range.

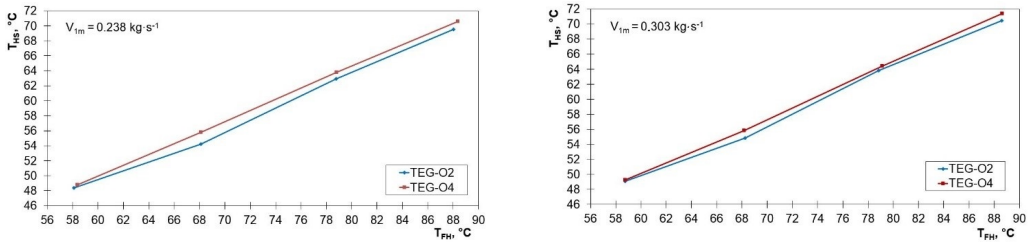

(**a**) (**b**)

Figure 10. Characteristics of the dependence of inlet and outlet temperatures for extreme effectiveness cases at different flows: (**a**) $V_{1m} = 0.238$ kg· s^{-1}; (**b**) $V_{1m} = 0.303$ kg· s^{-1}.

3.2. Distribution of Parameters along the HSHE

The efficiency of energy conversion in thermoelectric modules is related, on the one hand, to the uniform temperature distribution of the TEG hot side [20], and on the other hand to the highest temperature difference on the TEG walls. Thus, an optimal temperature distribution on the HSHE, according to the criteria mentioned above, will generate the greatest electric power of THM. In the experimental tests (Figures 11 and 12), the TEG-O2 circulation was characterized by the best parameters (the highest temperature difference on the walls and uniformity of its distribution along the HSHE), and TEG-O3 the weakest. The results were obtained with constant parameters of the fluid flow rate V_{1m} and the hot fluid inlet temperature of $T_{1in} = 69$ °C. The difference between the best case of circulation and the worst case was up to several °C.

A relatively uniform temperature distribution was achieved in TEG-O2 along the HSHE for each analyzed temperature range (Figure 12a).

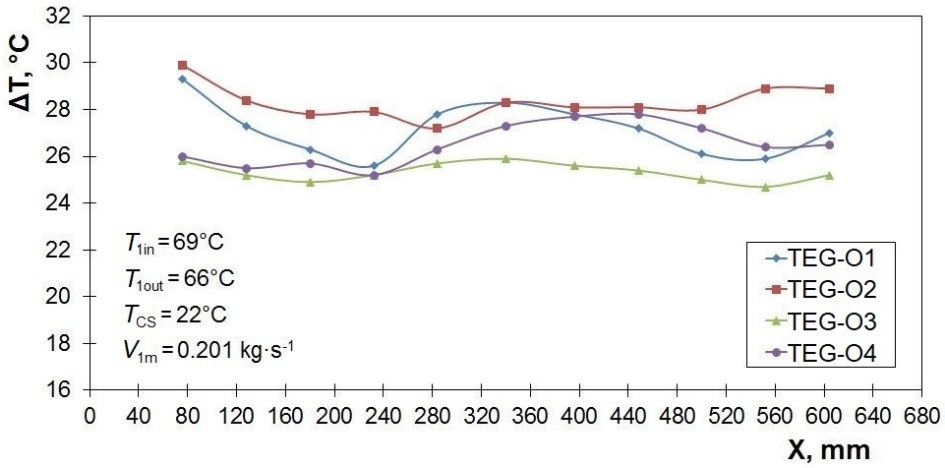

Figure 11. Distribution of the temperature difference along the surface of the HSHE in contact with the THM with different hot side fluid circuits.

The only uneven distributions occur at the ends of the exchanger, where the thermal energy is supplied to this liquid circuit. Hence, thermocouples should be placed in the middle of the HSHE, leaving the ends free. While TEG-O3 is characterized by a greater unevenness of the temperature distribution on the hot side (Figure 12b). This is due to the supply of thermal energy, two-section in reverse, to the circulation of the cold side. Thus, local temperature increases on the HSHE wall appear; however, the increases in T_{HS} do not result in an increase in the temperature difference and a greater generation of electricity in THM.

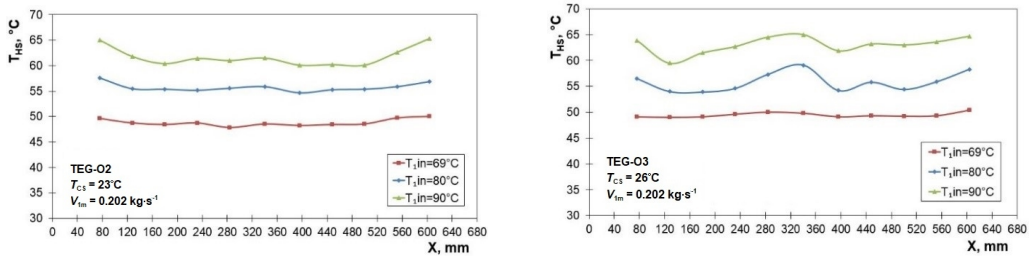

(**a**) (**b**)

Figure 12. Temperature difference distributions along the HSHE with varying supply temperatures, for the two selected circulations: (**a**) TEG-O2; (**b**) TEG-O3.

Figure 13 shows the actual results and approximate characteristics of the temperature distribution along the longer edge of the exchanger wall for parallel fluid flows: concurrent and counter-rotating, on the hot side of the HSHE.

The tendency of temperature changes on the exchanger walls is similar to that obtained in simulation studies in [18] for concurrent and counter-rotating flows. The linear regression of the raw data for TEG-O1 maps the nature of the temperature changes along the exchanger, where T_{HS} is a decreasing function and T_{CS} is an increasing function. For counter-rotating flows, the trends of the characteristics were similar to those of the results of the numerical model [18]. The determined approximated characteristics of T_{HS} and T_{CS} temperature changes along the longer edge of the exchanger in the TEG-O3 are linear increasing functions.

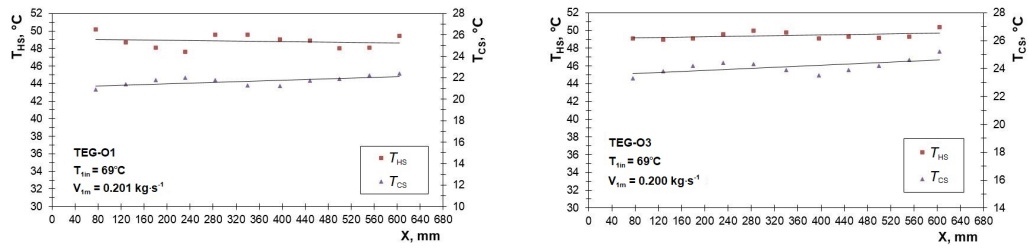

(**a**) (**b**)

Figure 13. Temperature changes on the hot and cold side of the parallel walls of the exchangers in contact with the TEG plates, with selected hot side fluid circulations: (**a**) TEG-O1; (**b**) TEG-O3.

3.3. Efficiency of Energy Conversion in the TEG Module

The experimentally determined temperature distributions allowed for the determination of the TEG operating parameters. A set of 20 series-connected TEGs with a maximum generated power of approx. 5W was used (Table 1). The equivalent electrical circuits for this system are shown in Figure 14.

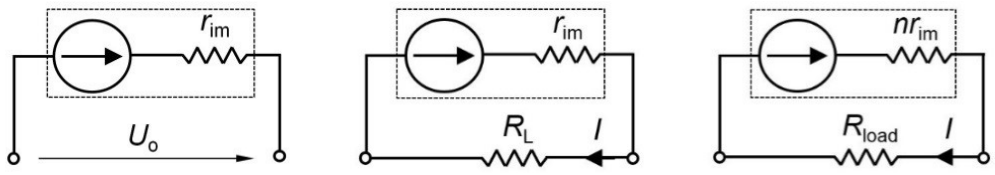

(**a**) (**b**) (**c**)

Figure 14. Equivalent electrical circuits of the TEG; (**a**) open circuit voltage; (**b**) closed circuit voltage (with load resistance of single TEG); (**c**) closed circuit voltage (with load resistance of n TEG).

The applied thermoelectric modules are characterized by a maximum operating temperature of the hot side equal to 138 °C. The voltage U_o generated in the open circuit of a single module (Figure 14a) is proportional to the temperature difference ΔT_m between the outer walls of the TEG:

$$U_o = N\alpha\Delta T_m \tag{2}$$

With the maximum power generated by the TEG and the assumption that the load resistance is equal to its internal resistance, the relationship is satisfied:

$$I_o = \frac{U_o}{r_{im} + R_L} \tag{3}$$

In the presented research, the results of the tests of the TEG set under the conditions of the open circuit of individual thermoelectric modules were not presented, as they were discussed in the article [20].

During the tests, the changes in the internal resistance of selected TEGs, modules a_{23} and a_{28}, located in the central parts of individual sections of the HSHE, were analyzed (Figure 5b). The experiment shows that the value of the internal resistance of TEG, at a constant temperature T_{1in} and a variable mass flow rate V_{1m}, increases, but to a slight extent. The average value of the internal resistance of a single TEG was determined based on the results of the tests of the two above-mentioned modules, which is $r_{im} = 0.608\ \Omega$ with a measurement uncertainty of $\pm 0.012\ \Omega$, at the temperature $T_{1in} = 90\ ^\circ\text{C}$ (Figure 15).

The expanded uncertainty was determined from the dependence on the complex uncertainty u_c (statistically and using the B method), with a confidence level of 95.45% [23,24], as below:

$$u_c^2 = (\frac{\partial f}{\partial I})^2 \cdot u_I^2 + (\frac{\partial f}{\partial U})^2 \cdot u_U^2 \tag{4}$$

where:

u_I—standard uncertainty of type A, current measurement,

u_U—standard uncertainty of type A, voltage measurement.

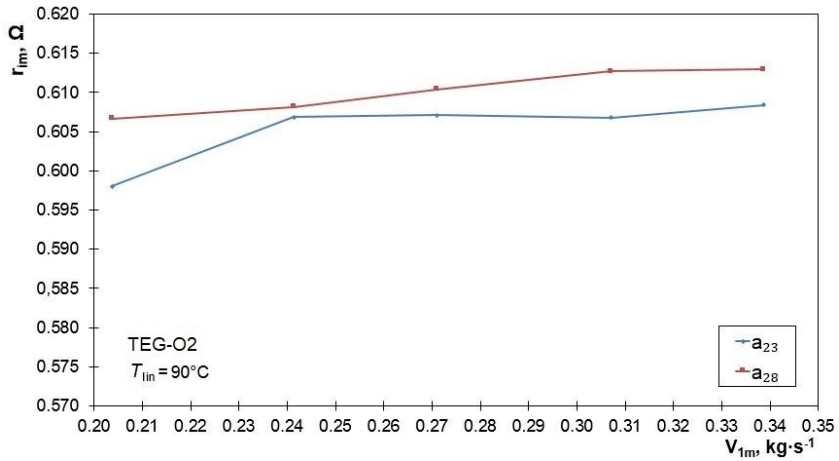

Figure 15. Characteristics of changes in the internal resistance of selected TEGs as a function of the flow rate V_{1m}.

The value of the voltage U_L on the load resistance R_L of a single TEG can be determined as follows:

$$U_L = IR_L \tag{5}$$

The value of the voltage U_{load} on the load resistance R_{load}, for n single TEG, is determined as follows:

$$U_{load} = IR_{load} \tag{6}$$

The power generated at the output of a single loaded TEG is:

$$P_{TEG} = I^2 R_L \tag{7}$$

while the power generated at the THM output of the analyzed loaded system is:

$$P_{THM} = I^2 R_{load} \tag{8}$$

The MTEG module, under the conditions of the experiment (for certain parameters: $V_{1m}, T_{1in}, \Delta T_m$), is able to generate P_{THM} power up to 28 W. The generated power increases with increasing the temperature T_{1in} at the inlet of HSHE and the hot fluid flow rate V_{lm} (Figure 16). The highest value of P_{THM} is achieved by the module at the maximum mass flow rate V_{1m}, the maximum temperature $T_{1in} = 90\,^{\circ}\mathrm{C}$, and the temperature difference on the walls of the TEG $\Delta T_m = 47\,^{\circ}\mathrm{C}$ (Figure 16b).

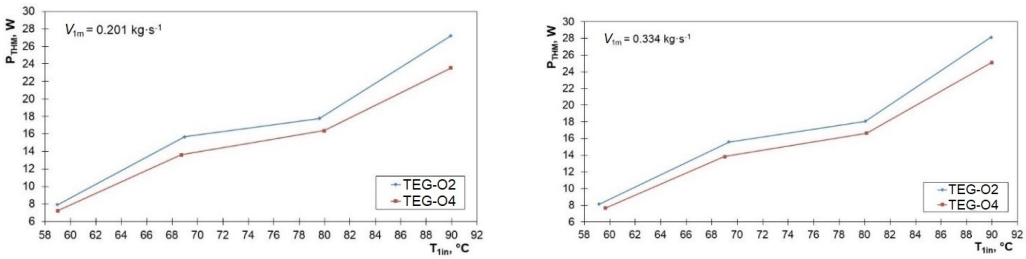

(**a**) (**b**)

Figure 16. Characteristics of the power generated by the TEG set in relation to T_{1in} at the minimum and maximum flow rate V_{1m} for the selected HSHE fluid circulations: (**a**) $V_{1m} = 0.201$ kg· s^{-1}; (**b**) $V_{1m} = 0.334$ kg· s^{-1}.

The circulation that gives the best power generation parameters in the THM system turns out to be the TEG-O2, which provides significantly better parameters. In the experiment, a high-power wire resistor with $R_{load} = 12\ \Omega$ was used as a load.

Thermodynamic analysis of the phenomena occurring in the thermoelectric module consists of taking into account four types of heat: Peltier cooling ($\dot{Q}_{PEC}, W$), Peltier heating ($\dot{Q}_{PEC}, W$), Fourier ($\dot{Q}_{FH}, W$), and Joule ($\dot{Q}_{JH}, W$) [25,26].

$$\dot{Q}_{PEC} = \alpha I T_{CS} \tag{9}$$

$$\dot{Q}_{PEH} = \alpha I T_{HS} \tag{10}$$

$$\dot{Q}_{FH} = k_T (T_{HS} - T_{CS}) \tag{11}$$

$$\dot{Q}_{JH} = I^2 r_{im} \tag{12}$$

Hence, the heat flux adsorbed by the hot junctions of the TEG set ($\dot{Q}_{HS}$) and flowing through the cold side of the THM ($\dot{Q}_{CS}$) is as follows:

$$\dot{Q}_{HS} = \dot{Q}_{FH} + \dot{Q}_{PEH} - \frac{1}{2}\dot{Q}_{JH} = k_T (T_{HS} - T_{CS}) + \alpha I T_{HS} - \frac{1}{2} I^2 r_{im} \tag{13}$$

$$\dot{Q}_{CS} = \dot{Q}_{FH} + \dot{Q}_{PEC} + \frac{1}{2}\dot{Q}_{JH} = k_T (T_{HS} - T_{CS}) + \alpha I T_{CS} + \frac{1}{2} I^2 r_{im} \tag{14}$$

Using the above dependencies, the efficiency of single TEGs can be determined, which relates to the heat flux $\dot{Q}_{HS}$ and the generated electric power. In turn, the efficiency of the entire MTEG η_{TEG} was determined on the basis of experimental studies, the generation of electric power by THM, and the heat flux supplied to the inlet of HSHE:

$$\eta_{TEG} = \frac{P_{THM}}{\dot{Q}_{1in}} \tag{15}$$

The highest MTEG efficiency for the temperature $T_{1in} = 69\,^{\circ}\mathrm{C}$ and the average difference $\Delta T_m = 27\,^{\circ}\mathrm{C}$, and the system achieves for the TEG-O2 circulation and the mass flow rateV_{1m} = 0.238 kg/s (Figure 17), similarly to the best effectiveness ε_{HSHE} of HSHE operation. The least effective circulations turn out to be TEG-O3 and TEG-O4.

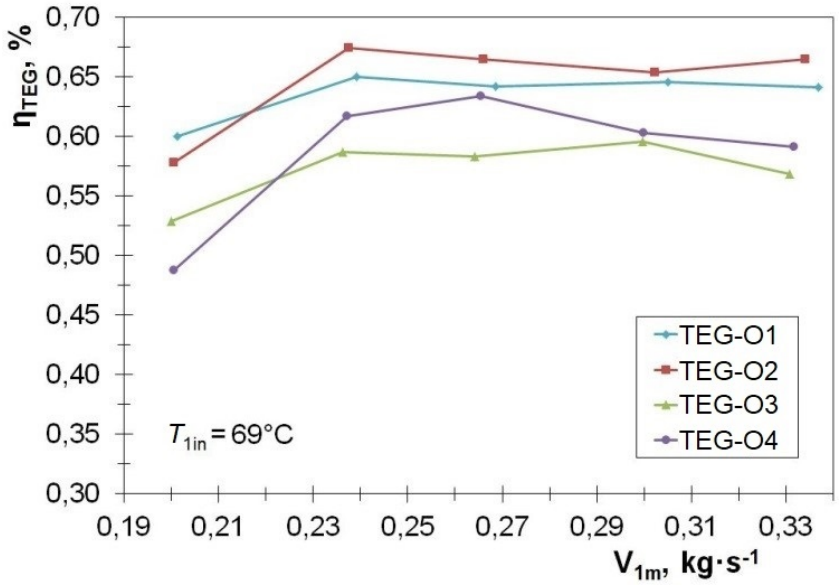

Figure 17. Efficiency characteristics of η_{TEG} at different flow rates and cycles of the MTEG hot side fluid and temperature $T_{1in} = 69\,^{\circ}\mathrm{C}$.

For elevated conditions of the experiment ($T_{1in} = 90\,^{\circ}\mathrm{C}$, $\Delta T_m = 47\,^{\circ}\mathrm{C}$) and constant temperature of the cold side, the MTEG efficiency is η_{TEG} = 0.93%, with a flow rate of V_{1m} = 0.238 kg/s and circulation TEG-O2 (Figure 18a). Similarly, TEG-O4 turned out to be less effective (Figure 18), and the increased flow rate did not improve the efficiency.

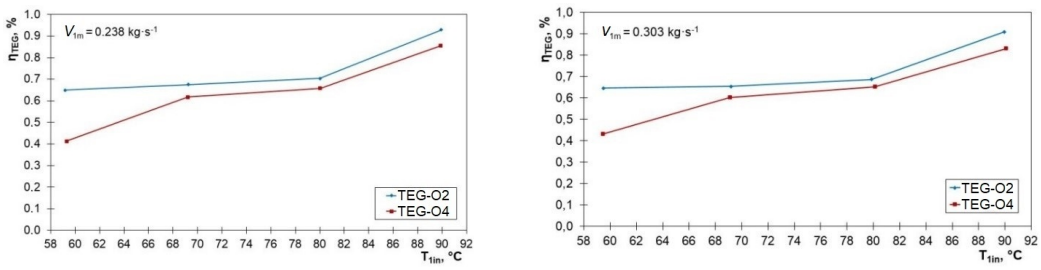

(**a**) (**b**)

Figure 18. Efficiency characteristics of η_{TEG} at different T_{1in} temperatures and selected flow rates: (**a**) $V_{1m} = 0.238\ \mathrm{kg}\cdot\mathrm{s}^{-1}$; (**b**) $V_{1m} = 0.303\ \mathrm{kg}\cdot\mathrm{s}^{-1}$.

The tests show that the efficiency of the system η_{TEG} increases with the increase of the temperature T_{1in} the hot fluid at the inlet of the exchanger. The highest efficiency is achieved with the mass flow equal to V_{1m} = 0.238 kg/s, and a further increase in the mass flow rate does not improve the system efficiency (Figure 18). It results from the fact that the maximum η_{TEG} in relation to the mass flow rate is about 0.238 kg/s (Figure 17).

Increasing the efficiency of the presented MTEG system is connected, on the one hand, with the determination of the optimal flow rate, and, on the other hand, with increasing the temperature of the hot side of HSHE. Nevertheless, the main limitation to further increasing the efficiency of η_{TEG} in real MTEG systems is the maximum allowable temperature of the hot side of the thermoelectric module used. In the analyzed system, it is at a low level, which results from the use of low-temperature heat for energy recovery.

4. Conclusions

The paper presents the results of experimental research on the influence of flow, thermal, and design parameters, and configuration of liquid circulation in HSHE on the power generated in the MTEG module and its efficiency. The analysis takes into account the determination of the main characteristics of the HSHE exchanger and the module's response to variable thermal and flow forces. The design of the MTEG is based on the hot and cold side flat liquid heat exchanger. The use of a two-section design of the hot side exchanger improves the efficiency of MTEG.

During the experiment, the behavior of HSHE was analyzed in four configurations of the hot side fluid circulation. The research shows that the TEG-O4 and TEG-O2 circulations are extreme configurations. The best is the circulation of the hot side exchanger with a parallel flow directed towards the center (TEG-O2), which in a two-section exchanger combines co-rotating flow (first section—$S1_H$) and counter-rotating flow (second section—$S2_H$). This circulation allows for achieving the best parameters, including the generation of electrical power. The highest effectiveness of ε_{HSHE} and efficiency of η_{TEG} were also obtained for this circulation. The generated electric power at the MTEG output increased by 14%, the efficiency by 16%, and the HSHE effectiveness by 7% in relation to the counter-current flow in both sections of the exchanger.

Hydraulic and thermal losses through connections and housings were not included in the analysis. These losses will be the subject of further analyzes, and their minimization may turn out to be significant in increasing the efficiency and performance parameters of the prototype device and its operation in real conditions.

Author Contributions: Conceptualization, methodology, validation, formal analysis, and investigation—M.N., M.M., M.Ż.-M., and A.M.; writing—original draft preparation, review and editing, M.N. and M.Ż.-M.; visualization—M.M. and A.M. All authors have read and agreed to the published version of the manuscript.

Funding: This research was funded from the targeted subsidy by Łukasiewicz Research Network—Institute for Sustainable Technologies in Radom, Grant No. 2/Ł-ITEE/CŁ/2021.

Institutional Review Board Statement: Not applicable.

Informed Consent Statement: Not applicable.

Conflicts of Interest: The authors declare no conflict of interest.

Abbreviations

The following abbreviations are used in this manuscript:

CSHE	cold side heat exchanger
HS	heat source
HSHE	hot side heat exchanger
MTEG	TEG grouped in modules
TEG	thermoelectric generators
THM	set of thermoelectric generators

Nomenclature

T_{1in}	initial liquid temperature, °C
T_{1out}	liquid outlet temperature, °C
T_{FH}	liquid temperature entering the HSHE, °C
T_{HS}	hot-side temperature, °C
T_{CS}	cold-side temperature, °C
ΔT_m	temperature difference between hot and cold side of the TEG module, °C
$\dot{Q}_{1in}$	heat flux entering the HSHE, W
$\dot{Q}_{1out}$	heat flux leaving the HSHE, W
$\dot{Q}_{HS}$	heat flux absorbed at the hot junction of the MTEG, W
$\dot{Q}_{CS}$	heat flux sank at the cold junction of the MTEG, W
P_p	power needs for pressure losses, W
P_{THM}	electrical power generated by the THM, W
α	Seebeck coefficient, V/K
U_o	voltage generated by the TEG, V
r_{im}	internal electrical resistance of the TEG, Ω
R_{load}	load resistance, Ω
I_o	current for the maximum power generated by the TEG, A
I	electrical current, A
N	number of couples in the TEG
V_{1m}	initial liquid mass flow rate, kg/s
n	number of the TEG in the THM
R_L	load resistance of the single TEG, Ω
ε_{HSHE}	HSHE effectiveness, %
η_{TEG}	MTEG efficiency, %
k_T	thermal conductance of the TEG, W/K
V_{CSHE}	flow rate in the CSHE, %
T_{CSHE}	initial liquid temperature in the CSHE, %

References

1. Jaziri, N.; Boughamoura, A.; Müller, J.; Mezghani, B.; Tounsi, F.; Ismail, M. A comprehensive review of Thermoelectric Generators: Technologies and common applications. *Energy Rep.* **2020**, *6*, 264–287. doi:10.1016/j.egyr.2019.12.011.
2. Twaha, S.; Zhu, J.; Yan, Y.; Li, B. A comprehensive review of thermoelectric technology: materials, applications, modeling and performance improvement. *Renew. Sustain. Energy Rev.* **2016**, *65*, 698–726. doi:10.1016/j.rser.2016.07.034.
3. Goupil, C.; Seifert, W.; Zabrocki, K.; Muller, E.; Snyder, G.J. Thermodynamics of Thermoelectric Phenomena and Applications. *Entropy* **2011**, *13*, 1481–1517. doi:10.3390/e13081481.
4. Machacek, Z.; Walendziuk, W.; Sotola, V.; Slanina, Z.; Petras, R.; Schneider, M.; Masny, Z.; Idzkowski, A.; Koziorek, J. An Investigation of Thermoelectric Generators Used as Energy Harvesters in a Water Consumption Meter Application. *Energies* **2021**, *14*, 3768. doi:10.3390/en14133768.
5. Quan, R.; Liu, G.; Wang, C.; Zhou, W.; Huang, L.; Deng, Y. Performance Investigation of an Exhaust Thermoelectric Generator for Military SUV Application. *Coatings* **2018**, *8*, 45. doi:10.3390/coatings8010045.
6. Rezania, A.; Rosendahl, L.A. Thermal effect of a thermoelectric generator on parallel microchannel heat sink. *Energy* **2012**, *37*, 220–227. doi:10.1016/j.energy.2011.11.043.
7. Rowe, D.M.; Min, G. Evaluation of thermoelectric modules for power generation. *J. Power Sources* **1998**, *73*, 193–198. doi:10.1016/S0378-7753(97)02801-2.
8. Goldsmid, H.J. Bismuth Telluride and Its Alloys as Materials for Thermoelectric Generation. *Materials* **2014**, *7*, 2577–2592. doi:10.3390/ma7042577.
9. Elsheikh, M.H.; Shnawah, D.A.; Sabri, M.F.M.; Said, S.B.M.; Hassan, M.H.; Bashir, M.B.A.; Mohamad, M. A review on thermoelectric renewable energy: Principle parameters that affect their performance. *Renew. Sustain. Energy Rev.* **2014**, *30*, 337–355. doi:10.1016/j.rser.2013.10.027.
10. Riffat, S.B.; Ma, X. Review thermoelectrics: A review of present and potential applications.*Appl. Therm. Eng.* **2003**, *23*, 913–935. doi:10.1016/S1359-4311(03)00012-7.
11. Zuazua-Ros, A.; Martin-Gomez, C.; Ibanez-Puy, E.; Vidaurre-Arbizu, M.; Gelbstein, Y. Investigation of the thermoelectric potential for heating, cooling and ventilation in buildings: Characterization options and applications. *Renew. Energy* **2019**, *131*, 229–239. doi:10.1016/j.renene.2018.07.027.

12. Zoui, M.A.; Bentouba, S.; Stocholm, J.G.; Bourouis, M. A Review on Thermoelectric Generators: Progress and Applications. *Energies* **2020**, *13*, 3606. doi:10.3390/en13143606.
13. Lv, S.; Qian, Z.; Hu, D.; Li, X.; He, W. A Comprehensive Review of Strategies and Approaches for Enhancing the Performance of Thermoelectric Module. *Energies* **2020**, *13*, 3142. doi:10.3390/en13123142.
14. Garud, K.S.; Seo, J.H.; Patil, M.S.; Bang, Y.M.; Pyo, Y.D.; Cho, C.P.; Lee, M.Y. Thermal–electrical–structural performances of hot heat exchanger with different internal fins of thermoelectric generator for low power generation application. *J. Therm. Anal. Calorim.* **2020**, *143*, 387–419. doi:10.1007/s10973-020-09553-7.
15. Crane, D.T.; Jackson, G.S. Optimization of cross flow heat exchangers for thermoelectric waste heat recovery. *Energy Convers. Manag.* **2004**, *45*, 1565–1582. doi:10.1016/j.enconman.2003.09.003.
16. Esarte, J.; Gao, M.; Rowe, D.M. Modelling heat exchangers for thermoelectric generators. *J. Power Sources* **2001**, *93*, 72–76.
17. Su, C.Q.; Zhan, W.W.; Shen, S. Thermal Optimization of the Heat Exchanger in the Vehicular Waste-Heat Thermoelectric Generations. *J. Electron. Mater.* **2012**, *41*, 1693–1697. doi:10.1007/s11664-012-2095-5.
18. Yu, J.; Zhao, H. A numerical model for thermoelectric generator with the parallel-plate heat exchanger. *J. Power Sources* **2007**, *172*, 428–434. doi:10.1016/j.jpowsour.2007.07.045.
19. Łęcki, M.; Andrzejewski, D.; Gutkowski, A.N.; Górecki, G. Study of the Influence of the Lack of Contact in Plate and Fin and Tube Heat Exchanger on Heat Transfer Efficiency under Periodic Flow Conditions. *Energies* **2021**, *14*, 3779. doi:10.3390/en14133779.
20. Mrozek, M.; Majcher, A. Application of thermoelectric generators for electrical energy production with a low-temperature heating source. *J. Mach. Constr. Maint. Probl. Eksploat.* **2017**, *4*, 123–130.
21. Hebei, TEC1-12730 Datasheet. Available online: http://www.hebeiltd.com.cn/peltier.datasheet/TEC1-12730.pdf (accessed on 8 June 2021).
22. European Commission Directorate-General For Energy, Directorate C. 2—New Energy Technologies, Innovation and Clean Coal: Mapping and Analyses of the Current and Future (2020–2030) Heating/Cooling Fuel Deployment (Fossil/Renewables). Final Report. September, 2016. Available online: https://irees.de/wp-content/uploads/2021/01/Scenarios-for-heating-cooling-demand-and-supply.pdf (accessed on 28 February 2017).
23. Evaluation of Measurement Data—Guide to the Expression of Uncertainty in Measurement. JCGM 100:2008. Available online: https://www.bipm.org/documents/20126/2071204/JCGM_100_2008_E.pdf/cb0ef43f-baa5-11cf-3f85-4dcd86f77bd6 (accessed on 2 July 2021).
24. Neska, M.; Majcher, A. Estimation of the uncertainty of measurement in a two-channel system for tests on the intensity of infrared radiation. *Probl. Eksploat. Maint. Probl.* **2014**, *3*, 45–55.
25. Irshad, K.; Habib, K.; Thirumalaiswamy, N.; Saha, B.B. Performance analysis of a thermoelectric air duct system for energy-efficient buildings. *Energy* **2015**, *91*, 1009–1017. doi:10.1016/j.energy.2015.08.102.
26. Kin, L.K.; Baheta, A.T.; Habib, K. Analytical Investigation of Thermoelectric Performance for Cooling Application. *J. Adv. Res. Fluid Mech. Therm. Sci.* **2018**, *46*, 32–40.